Accepted manuscript of the article published in
International RILEM Conference on Synergising Expertise towards Sustainability and Robustness of Cement-based Materials and Concrete Structures, SynerCrete'23 - Volume 2,
part of the RILEM Bookseries (RILEM, volume 44), pp 665-672.
The final publication is available at Springer via https://doi.org/10.1007/978-3-031-33187-9_61

An optimum mix design method for 3D concrete printing applications

Sergis, Vasileios[1[002-7743-470X.]] and Ouellet-Plamondon, Claudiane[1[0003-3795-4791]]

[1] École de technologie supérieure, Université du Québec, Montréal, QC, H3C 1K3, Canada
Claudiane.Ouellet-Plamondon@etsmtl.ca

Abstract. Developing cement-based mortar mixes for three-dimensional printing applications is a challenging task with multiple competing objectives, especially with climate change adaptation. Mortar mix design is a laboratory method that determines the necessary quantities and types of cement, sand, chemical admixtures, and water to form a combination with the specified qualities. The influx of new ingredients to investigate can lead to an inefficient amount of labour. This research is part of a bigger project aiming to automate the development of mortar mixtures for three-dimensional concrete printing technology. A party optimizer suggests novel combinations by adjusting the ingredients and their proportions, whereas feed-forward neural networks predict their properties. In total, seven factors are investigated, five of which are quantitative and two qualitative. These factors include the type of cement and superplasticizer used, as well as the sand-to-binder ratio, water-to-binder ratio, and admixture doses. The initial set of mixes formed in the laboratory derived from a D-optimal set of 18 mixes. Tests frequently used in traditional construction are conducted to correlate them with important properties for 3D concrete printing applications. The flow table test correlates with flowability, whereas the slump test correlates with shape stability. The mixtures with the desired properties are then tested with the extrusion system, which includes a progressive cavity pump and an extrusion head. This is an ongoing study also including lower carbon mixes and it is expected that as the number of iterations increases, so will the qualities of the mixtures according to the given design criteria.

Keywords: 3D printing, cement, admixtures, mix design, optimization algorithms.

1 Introduction

When looking for solutions to adapt to climate change, prior knowledge on mortar mixes have an important role in mix design. In many studies the mixture proportion is given directly, with no design method or explanation of how the parameters were obtained. Various techniques are being used where the most popular ones being the trial and error process, change one factor at the time, or following a full-factorial design [1-3]. In 3D concrete printing applications, the property of the mixtures during the fresh state is crucial. The mixture should be pumpable, extrudable, able to keep its shape once deposited and able to withstand the weight of the additional layers without deforming or collapsing [4-10]. This adds to the complexity in the mix design process where compared to the mixtures formed in the traditional construction [11]. The various available options of ingredients that can be added in the mix design often leads to mix designs with high complexity. As the number of the factors and their levels are increased the number of experiments can become an onerous task to fulfil [12-14]. Many researchers opt to concentrate on a few factors of the mixture while focusing the majority of their attention on specific ingredients of the mixes, such as chemical admixtures and their dosages. As a result, the main compositions of the mix, such as cement, sand, or water, remain constant. This study attempts to accelerate the development of new mixtures for 3D printing applications while investigating complex mix designs. This research is part of a bigger project aiming to later include lower carbon mixes to adapt to climate change. Initially, it gathers information on numerous factors of a complex mix design using a design of experiments (DoE) method. Part of the experiments are simulated while using optimization algorithms to guide the process and feedforward neural networks to estimate the properties of the mixtures. Artificial intelligence has been used in many studies in civil engineering [15-17]. The printable and buildability region of the mixtures can be defined using two popular tests in the construction field, the slump and flow test [8].

2 Materials, testing methods and methodology

2.1 Materials

The selected ingredients are five admixtures, including the superplasticizers, and three types of cement. Fine sand with particle sizes below 2.5 mm is used [18, 19]. The three admixtures are a biopolymer polysaccharide viscosity modifying agent (B), a water-reducing-non-chloride accelerating admixture (A), and a calcium silicate hydrate admixture (CSH-C). Both superplasticizers selected are based on synthetic organic polymers (PCE 1 & 2). For cement, the three types are binary cement with silica fumes (GUbSF), general use Portland cement blended with limestone (GUL), and Portland cement with a high early strength (HE).

2.2 Testing methods

All the selected tests are conducted in the dormant period of the mortar mixtures. The ASTM C1437 flow test is used to measure the spread of the mixes and to correlate the results with the pumpability of the mixes. These measurements can ensure that there will be no clogging while transferring the material from the pump towards to the outlet of the extruder. The flow target was to achieve a spread of at least 115 % [8] 5 minutes after the mixing process. Tests were conducted after 5, 15 and 30 minutes. Two cameras were placed, capturing a side and the top view, to inspect the behaviour of each mixture over time (Fig. 1a). The ASTM C143 slump test provided an insight on the behaviour of the mixture related to its shape stability. The mini-slump cone is used with dimensions of 150 mm x 100 mm x 50 mm height, base and top diameter respectively. Tests were conducted after 5, 15 and 30 minutes (Fig. 1b, c, and d).

Fig. 1. Top view of the flow table (a), side view of the slump test (b, c, d).

Finally, the ASTM D3080 direct shear test is used to observe the strength development of the mixture during the dormant period. Multiple tests are conducted within 90 minutes following a similar methodology where the same test was performed [5, 6]. The main components of the direct shear apparatus are a linear displacement motor and a shear box. For this study the apparatus is modified by adding a displacement sensor and a load sensor to capture the strength development of the mixture. An illustration of the equipment is shown in Fig. 2.

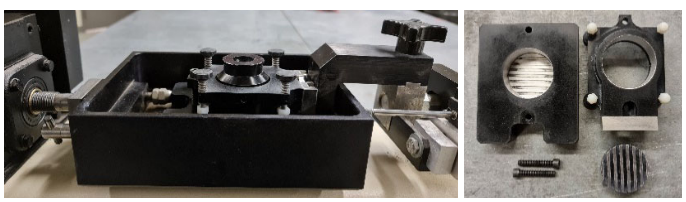

Fig. 2. The direct shear apparatus (a), and the shear box (b).

2.3 Extrusion system

The 3D concrete printer used in this study utilizes a 6-DOF robot manipulator, a progressive cavity pump, and an extrusion head. The robot manipulator is the IRB6700 from ABB, and it has a working envelope of 3.2 m and a maximum load of 150 kg. The progressive cavity pump can deliver highly viscous and thixotropic mixtures with accuracy and repeatability. The extrusion head (fig. 3b) consists of an auger screw to convey and deposit the material through the nozzle. The motors at the pump and the extrusion head are calibrated to give the desired constant flow using variable frequency drives. Temperature and pressure sensors are added as a feedback subsystem to monitor the printing process. The large-scale additive manufacturing laboratory of ETS is depicted in Fig. 3.

Fig. 3. The large-scale additive manufacturing laboratory of ETS and the extrusion system used in this study (a), the extrusion head (b), and the progressive cavity pump (c).

2.4 Methodology

To reduce the number of mixes to be formed in the laboratory, an initial set of mixes were selected using a design of experiment methodology. An optimal subset of 18 mixes were selected following a D-optimal design as in our previous study [19]. After the initial set, a multiobjective Pareto optimizer guides the procedure by proposing new combinations of the ingredients and their dosages [20]. Up to seven factors can be edited by the algorithm; of these, two are handled as qualitative factors and the other five as quantitative ones. The type of superplasticizers and the type of cement are the qualitative parameters. The quantitative factors include the ratios of water and sand to the binder, as well as the dosages of superplasticizer, biopolymer polysaccharide viscosity modifier, water-reducing-non-chloride accelerating admixture, and crystalline calcium silicate hydrate. Feedforward artificial neural networks are trained using data from lab experiments, and they are updated in every iteration of the process. These networks are used to predict the properties of the new proposed mixtures during the optimization procedure. The final set of party front mixtures are formed and tested in the laboratory to acquire the real fresh and final properties of the mixtures. The objectives are to increase simultaneously the buildability and the shape stability of the mixes, while acquiring an acceptable flowability.

3 Results

During the printing process, the plastic collapse of the printed structure was observed due to inadequate strength of the mix (Fig. 4a), and the elastic bulking due to inadequate stability of the mix (Fig. 4b). Those are two failure mechanisms which are often observed in 3D concrete printing [21]. The images of Fig. 4 were captured during the printing process from a camera placed near the printing area. Multiple tests have been made with adjusting the printing speed or the layer cycle time. The two examples in Figure 4, had a layer cycle time of 6 seconds with 38 layers being deposited before collapsing, and the Figure 4b, had a layer cycle time of 12 seconds with 19 layers being deposited before collapsing.

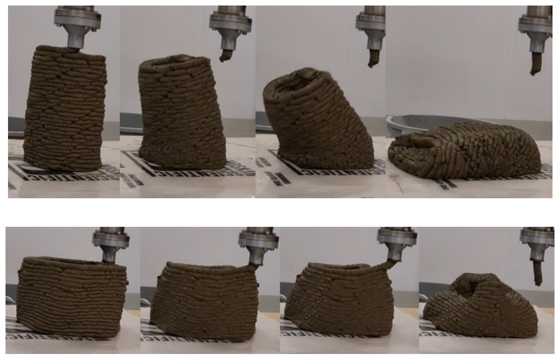

Fig. 4. Plastic collapse (a), and elastic buckling failure (b).

Six new mixes are introduced after two iterations of the Pareto optimization process. So far, 24 mixes are formed, including the initial set of mixes from the D-optimal design. All the new proposed mixes include the GUL cement type, the admixtures A, and CSH-C. The results obtained are shown in Fig. 5 and Fig. 6. The results are illustrated in two-dimensional figures with the flow, slump or yield stress of the mixes. The initial mixes are represented with hollow markers whereas the mixes proposed during the optimization process are shown with filled markers.

In Fig. 5a, the x-axis is the slump test and the y-axis is the flow test, both at 5 minutes after the mixing process. Aiming to improve both properties, the best mixes are located in the top left corner of the figure. As it can be noticed, there is always a compromise between the two properties. Four out of the six optimized mixes had a slump less than 4 cm. The x-axis and the y-axis of Fig. 5b are the shear stress at 90 minutes after the mixing process and the flow test at 5 min, respectively. Aiming to increase both properties, the best mixes are located in the top right corner of the figure. Five out of the six proposed mixes have a yield stress above 11 kPa. Finally, in Fig. 5c, the x-axis is the yield stress and the y-axis is the slump test, at 90 and 5 minutes after the mixing process respectively. With the goal to increase the yield stress but reduce the slump, the best mixes are located in the bottom right corner of the figure. Three of the proposed mixes have the best performance among the 24 formed mixes.

The flow of the mixes has been defined to be above 115%~120% during the calibration of the extrusion system. Hence, the area of interest of the flow in our study is between 115% to 135%. As mentioned previously, with the aim to increase the yield stress and reduce the slump, the results can be illustrated in a two-dimensional graph with the ratio of the yield strength and slump of the mixes. In Fig. 6a, the results are summarized in one graph focused in the area of interest. The best mixes are located in the right side of the figure. After only two iterations of the party optimization methodology, there is already one proposed mixture that outperforms the initial set of mixes. In Fig. 6b a few of the printed structures are presented with adequate buildability. One of the mixes had a layer cycle time of printed 6 seconds and it was possible to reach 54 layers. Not all of the mixes proposed by the party optimization algorithm have been tested while this manuscript is written.

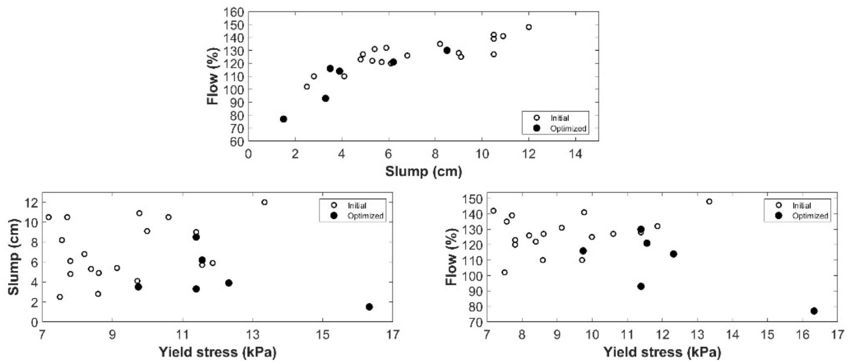

Fig. 5. Comparison between the initial and optimized mixes among the three investigated properties. Flow-slump (a), flow-yield stress (b), and slump-yield stress (c) of the 24 formed mixes. The measured yield stress is 90 minutes after mixing, whereas the flow and the slump is 5 minutes after mixing.

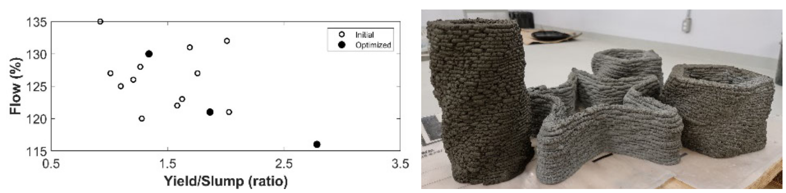

Fig. 6. Comparison between the initial and optimized mixes in the area of interest. The flow and yield/slump ratio are illustrated to summarize the results in a two-dimensional graph (a). Printed structures that succeeded the tests (b).

4 Conclusion

With this approach, less labour may be required to develop mixtures with enhanced properties. Statistics, optimization algorithms, and artificial intelligence all play an important role. This research is part of a bigger project aiming to automate the development process of 3D concrete printing mixtures to adapt to climate change. The suggested approach pursues a multiobjective party optimization trend while attempting to enhance the properties of the mixtures. In an effort to reconcile the competing goals, the optimizer determines the most crucial components and their optimal ratios. The slump test correlates with form stability, while the flow table test correlates with flowability. As the number of iterations rises, it is anticipated that the mixes will continue to be improved in this ongoing study. This method promises to enhance the conflicting goals of the mortar mixtures by drastically reducing the time and quantity of experiments needed.

Acknowledgments

This study is supported by Master Builders, Mitacs Acceleration, the Canada Research Chair program and the Canadian Foundation for Innovation. Sofoklis Giannakopoulos is gratefully acknowledged for his collaboration in fabricating the extrusion system.

References

[1] T. Ding, J. Xiao, S. Zou, and Y. Wang, "Hardened properties of layered 3D printed concrete with recycled sand," *Cement and Concrete Composites,* vol. 113, 2020, doi: 10.1016/j.cemconcomp.2020.103724.

[2] R. A. Buswell, W. R. Leal de Silva, S. Z. Jones, and J. Dirrenberger, "3D printing using concrete extrusion: A roadmap for research," *Cement and Concrete Research,* vol. 112, pp. 37-49, 2018, doi: 10.1016/j.cemconres.2018.05.006.

[3] F. Bos, R. Wolfs, Z. Ahmed, and T. Salet, "Additive manufacturing of concrete in construction: potentials and challenges of 3D concrete printing," *Virtual and Physical Prototyping,* vol. 11, no. 3, pp. 209-225, 2016, doi: 10.1080/17452759.2016.1209867.

[4] K. Ghafor, W. Mahmood, W. Qadir, and A. Mohammed, "Effect of Particle Size Distribution of Sand on Mechanical Properties of Cement Mortar Modified with Microsilica," *ACI Materials Journal,* vol. 117, no. 1, 2020, doi: 10.14359/51719070.

[5] R. J. M. Wolfs, F. P. Bos, and T. A. M. Salet, "Triaxial compression testing on early age concrete for numerical analysis of 3D concrete printing," *Cement and Concrete Composites,* vol. 104, 2019, doi: 10.1016/j.cemconcomp.2019.103344.

[6] R. J. M. Wolfs, F. P. Bos, and T. A. M. Salet, "Early age mechanical behaviour of 3D printed concrete: Numerical modelling and experimental testing," *Cement and Concrete Research,* vol. 106, pp. 103-116, 2018/04/01/ 2018, doi: https://doi.org/10.1016/j.cemconres.2018.02.001.

[7] R. Jayathilakage, J. Sanjayan, and P. Rajeev, "Direct shear test for the assessment of rheological parameters of concrete for 3D printing applications," *Materials and Structures,* vol. 52, no. 1, 2019, doi: 10.1617/s11527-019-1322-4.

[8] Y. W. D. Tay, Y. Qian, and M. J. Tan, "Printability region for 3D concrete printing using slump and slump flow test," *Composites Part B: Engineering,* vol. 174, 2019, doi: 10.1016/j.compositesb.2019.106968.

[9] P. Shakor, J. Renneberg, S. Nejadi, and G. Paul, "Optimisation of Different Concrete Mix Designs for 3D Printing by Utilizing 6DOF Industrial Robot," presented at the Proceedings of the 34th International Symposium on Automation and Robotics in Construction (ISARC), 2017.

[10] A. V. Rahul, M. Santhanam, H. Meena, and Z. Ghani, "3D printable concrete: Mixture design and test methods," *Cement and Concrete Composites,* vol. 97, pp. 13-23, 2019, doi: 10.1016/j.cemconcomp.2018.12.014.

[11] D. Marchon, S. Kawashima, H. Bessaies-Bey, S. Mantellato, and S. Ng, "Hydration and rheology control of concrete for digital fabrication: Potential admixtures and

cement chemistry," *Cement and Concrete Research,* vol. 112, pp. 96-110, 2018/10/01/ 2018, doi: https://doi.org/10.1016/j.cemconres.2018.05.014.

[12] M. Cavazzuti, *Optimization Methods: From Theory to Design. Scientific and Technological Aspects in Mechanics*. 2013.

[13] J. Lawson, *Design and Analysis of Experiments with R*. CRC Press Taylor & Francis Group, 2015.

[14] M. Charrier, Ouellet-Plamondon C., "Artificial neural network for the prediction of the fresh properties of cementitious materials," *Cement and Concrete Research,* 2019.

[15] K. T. Ateş, C. Şahin, Y. Kuvvetli, B. A. Küren, and A. Uysal, "Sustainable production in cement via artificial intelligence based decision support system: Case study," *Case Studies in Construction Materials,* vol. 15, 2021, doi: 10.1016/j.cscm.2021.e00628.

[16] S. Paul, B. Panda, H.-H. Zhu, and A. Garg, "An Artificial Intelligence Model for Computing Optimum Fly Ash Content for Structural-Grade Concrete," *ASTM International,* vol. 8, pp. 1-15, 01/14 2019, doi: 10.1520/ACEM20180079.

[17] Y. Pan and L. Zhang, "Roles of artificial intelligence in construction engineering and management: A critical review and future trends," *Automation in Construction,* vol. 122, 2021, doi: 10.1016/j.autcon.2020.103517.

[18] V. Sergis and C. M. Ouellet-Plamondon, "Fractional factorial design to study admixtures used for 3D concrete printing applications," *Materials Letters* vol. Submitted, 2022.

[19] V. Sergis and C. M. Ouellet-Plamondon, "D-optimal design of experiments applied to 3D high-performance concrete printing mix design," *Materials & Design* vol. Submitted 2022.

[20] V. Sergis and C. M. Ouellet-Plamondon, "Automating mix design for 3D concrete printing using optimization methods," *Digital Discovery,* 10.1039/D2DD00040G 2022, doi: 10.1039/D2DD00040G.

[21] R. Wolfs, S. Lucas, and T. A. M. Salet, "Elastic buckling and plastic collapse during 3D concrete printing," *Cement and Concrete Research,* vol. 135, p. 106016, 09/01 2020, doi: 10.1016/j.cemconres.2020.106016.